$N^*(1520)$ transition form factors from dispersion theory

Di An*

[1]Institutionen för fysik och astronomi, Uppsala universitet, Box 516, S-75120 Uppsala, Sweden

Abstract. The electromagnetic transition form factors (TFFs) of the nucleon provide important information on the internal structure of hadrons. A model-independent dispersive calculation of the electromagnetic TFFs $N^*(1520) \to N$ at low energies is presented. Taking pion rescattering into consideration, we derived dispersive relations for the $N^*(1520) \to N$ TFFs that relate space-like and time-like regions from the first principles. Based on the space-like data from JLab and hadronic data measured by HADES, we make predictions for TFFs in the time-like region. Our predictions can be tested in future experiments (e.g. HADES).

1 Introduction

The electromagnetic form factors (FF) and transition form factors (TFFs) provide important information on the internal structure of nucleons and their excited states. At very high energies, perturbative QCD can be applied to gain the asymptotic behavior of both the elastic and transition FFs but at low and intermediate energies, perturbative methods fail to converge due to the growth of the QCD coupling constant. Even though, on the theory side, significant progress in the past decades has been made [1, 2], a model-independent prediction for the TFFs at low energies $|q^2| < 1$ GeV^2 which is dominated by the meson cloud contributions, is still lacking. To fill in this gap, based on dispersive formalism that includes the $\pi\pi$ rescattering effects in the s-channel and nucleon and Δ exchange in the t/u channel, we, for the first time, calculate the $N^*(1520) - N$ transition FFs in both space-like and time-like region for $|q^2| \leq 1$ GeV^2. On the experimental side, the space-like FFs have been measured by Jefferson lab (e.g.[3]) and the time-like FFs have been extracted by the HADES experiment [4], which offers interesting opportunities for a complete understanding of the low-energy TFFs.

2 Dispersive formalism

The $N^*(1520)$ has isospin $I = 1/2$ and $J^P = 3/2^-$. The electromagnetic matrix element is given by

$$\langle N|j_\mu|N^*\rangle = e\, \bar{u}_N(p_N)\, \Gamma_{\mu\nu}\, u^\nu_{N^*}(p_{N^*}) \qquad (1)$$

*e-mail: di.an@physics.uu.se

with

$$\Gamma^{\mu\nu} := i\left(\gamma^\mu q^\nu - \not{q} g^{\mu\nu}\right) m_N F_1(q^2) + \sigma^{\mu\alpha} q_\alpha q^\nu F_2(q^2) + i\left(q^\mu q^\nu - q^2 g^{\mu\nu}\right) F_3(q^2)\,, \quad (2)$$

where $q^\mu := p^\mu_{N^*} - p^\mu_N$ and F_i with $i = 1, 2, 3$ are constraint-free FFs that are suitable for dispersive calculations. The dispersive method has been used by Uppsala Group [5–7] to study the nucleon and hyperon FFs and in this work, we focus on the $N^*(1520)$ which is isovector dominant at low energies [8]. Diagrammatically, the FFs F_i, which are fully non-perturbative objects, are represented by the grey blob in Eq. (3). At low energies, the grey blob can be approximated by the right-hand diagram of Eq. (3). We saturate the grey blob by a pion-pair because from the vector-meson dominance point of view, the ρ meson couples strongly to the isovector TFF.

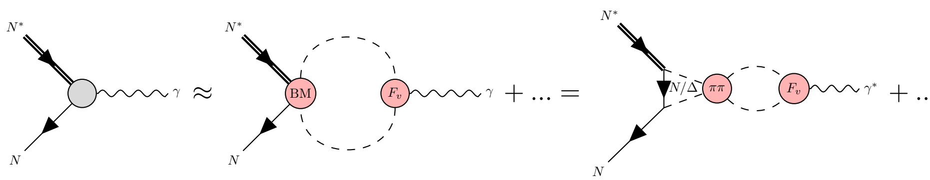

(3)

The red blob BM contains the $N^*(1520)\bar{N} \to 2\pi$ **b**aryonic and **m**esonic interactions and the FF can be further approximated by the second equality in Eq. (3) where the nucleon and Δ exchange in the crossing channels are explicitly shown. The Δ exchange has been shown to be important in FF calculations both in phenomenology and in the large N_c limit [6]. The F_v blob represents the pion-vector FF given by [6]

$$F_v(s) = (1 + \alpha_V\, s)\,\Omega(s) \quad (4)$$

with $\alpha_V = 0.12\,\mathrm{GeV}^{-2}$ and the Omnes function is $\Omega(s)$ defined as

$$\Omega(s) = \exp\left\{ s \int_{4m_\pi^2}^{\infty} \frac{\mathrm{d}s'}{\pi}\, \frac{\delta(s')}{s'\,(s' - s - i\epsilon)} \right\}, \quad (5)$$

where $\delta(s)$ is the p-wave pion phase shift. As already stressed, the dispersion relations are formulated for the constraint-free FFs [5]:

$$F_i(q^2) = \frac{1}{12\pi} \int_{4m_\pi^2}^{\infty} \frac{ds}{\pi}\, \frac{T_i(s)\, p^3_{\mathrm{cm}}(s) F_v^*(s)}{s^{1/2}\,(s - q^2 - i\epsilon)} + F_i^{\mathrm{anom}}(q^2) + \ldots \quad (6)$$

where $T_i(s) \sim \left\langle 2\pi \middle| N^* \bar{N} \right\rangle$ represents the hadronic p-wave partial wave amplitudes which are calculated using the following equation

$$T_i(s) = K_i(s) + \Omega(s)\, P_i + T_i^{\mathrm{anom}}(s) + \Omega(s)\, s \int_{4m_\pi^2}^{\infty} \frac{\mathrm{d}s'}{\pi}\, \frac{K_i(s')\, \sin\delta(s')}{|\Omega(s')|\,(s' - s - i\epsilon)\, s'}\,, \quad (7)$$

where K_i are the tree-level diagrams as input. $P_{i=1,2,3}$ are subtraction constants which are essentially fit parameters. They parametrize the short-distance physics that is not explicitly included in our low-energy theory. The subtraction constants

P_i are fitted by matching to the S and D-wave decay widths $N^*(1520) \to N\rho$ [8]. The peculiar contributions $F_i^{\text{anom}}(q^2)$ in Eq. (6) and $T_i^{\text{anom}}(s)$ in Eq. (7) originate from the anomalous cut in the first Riemann sheet. This anomalous cut rooted mathematically in the Landau equations has been discussed recently (e.g. see [5] and references therein).

3 Preliminary results and outlook

The isovector FFs are defined as $\frac{1}{2}(F_i^{\text{proton}} - F_i^{\text{neutron}})$. Based on the fitted subtraction constants $P_{1,2,3}$ introduced in Eq. (7), space-like FFs are calculated as shown in Fig. 1 where the experimental parametrizations are also presented. Our preliminary result shows nice agreement with the experimental parametrizations for $0 < Q^2 \le 0.4\,\text{GeV}^2$ with $Q^2 := -q^2$. However, due to the fact that the MAID neutron parametrization has relatively large systematic uncertainty [9], we want to stress[1] that the red curves should only be taken with a grain of salt. Time-like FFs are shown in

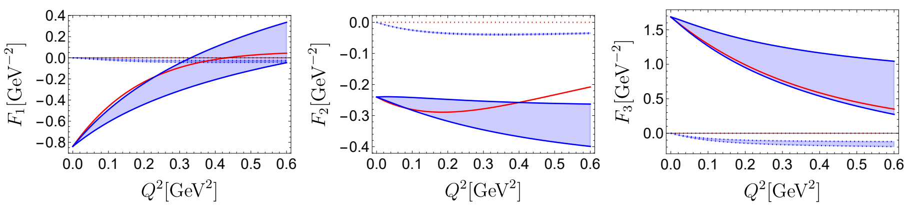

Figure 1: Red: Model dependent parametrization for isovector TFFs. We use Lisbon parametrization [10] for proton, MAID parametrization for neutron. Blue: this work (preliminary). Full lines: real part, Dashed lines: imaginary part.

Fig. 2. From the above predictions, differential decay widths $d\Gamma_{N^*\to Nl^+l^-}/dq$ and

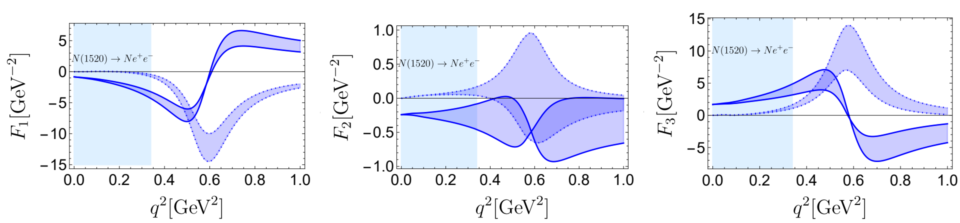

Figure 2: Time-like transition FFs (preliminary). Full lines: real part, dashed lines: imaginary part. The experimentally accessible region is defined as $q^2 \in [4m_e^2, (m_N - m_{N^*})^2]$ which corresponds to the light blue shaded area.

$d\Gamma_{N^*\to Nl^+l^-}/d\cos(\theta)$ are shown in Fig. 3. The preliminary results for Dalitz decay widths are $\Gamma_{Ne^+e^-} = 4.9 \pm 0.3\,\text{keV}$, $\Gamma_{N\mu^+\mu^-} = 0.85 \pm 0.25\,\text{keV}$. These numbers are larger than the QED estimates $\Gamma^{\text{QED}}_{Ne^+e^-} = 4.4\,\text{keV}$, $\Gamma^{\text{QED}}_{N\mu^+\mu^-} = 0.4\,\text{keV}$, due to the influence of ρ meson. These predictions can be tested by future experiments such as

[1]Especially, for F_2 at low energies the data parametrization shows that there is a broad dip which is probably due to systematic errors. Future measurements on the neutron TFFs will help to accurately extract the isovector TFFs and clarify the issue.

HADES and CBM [11]. In our dispersive framework, the only quantitative inputs are the S and D-wave $\Gamma_{N\rho}$ decay widths together with the hadronic two-body decay widths from $N^*(1520) \to N\pi, \Delta\pi$, which are the sources of uncertainties for our dispersive calculations. The uncertainties of the hadronic widths are propagated to our dispersive calculations, indicated by the bandwidths in Fig. 1, 2 and 3. Our dispersive calculations will certainly benefit from a more precise measurement of those quantities in the future.

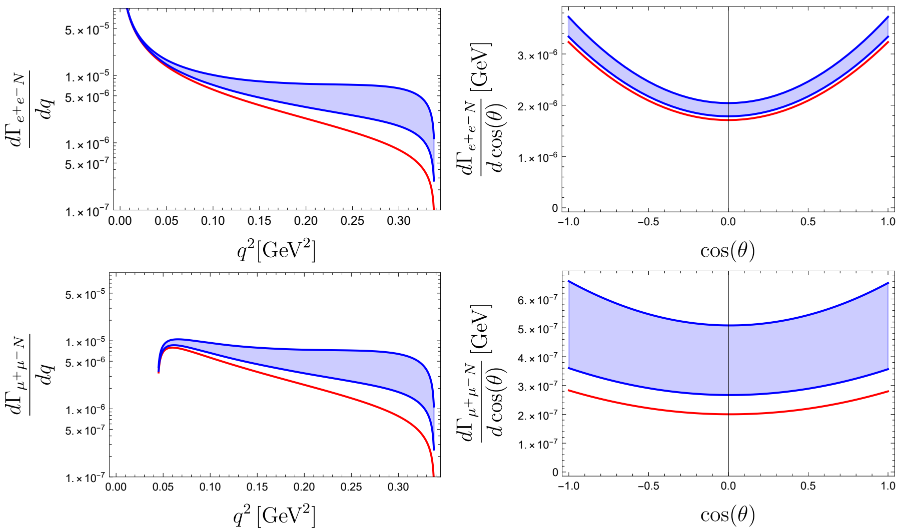

Figure 3: Predictions for electronic and muonic differential decay width (preliminary). The red curves are QED predictions. $q := \sqrt{q^2}$ and $\cos(\theta)$ is the angle between the outgoing nucleon and the lepton l^- in the virtual photon's rest frame.

4 Acknowledgements

This work has been supported by the Swedish Research Council (Vetenskapsrådet) (grant number 2019-04303). The author wants to acknowledge Liljewalch's travel scholarship for financing his attendance at the MESON 23 conference.

References

[1] G. Eichmann et al., Prog. Part. Nucl. Phys. **91**, 1 (2016)

[2] G. Ramalho, M.T. Peña (2023), `2306.13900`

[3] I.G. Aznauryan et al., Int. J. Mod. Phys. E **22**, 1330015 (2013)

[4] R. Abou Yassine et al. (HADES) (2022), `2205.15914`

[5] O. Junker, S. Leupold, E. Perotti, T. Vitos, Phys. Rev. C **101**, 015206 (2020)

[6] S. Leupold, Eur. Phys. J. **A54**, 1 (2018)

[7] C. Granados, S. Leupold, E. Perotti, Eur. Phys. J. **A53**, 117 (2017)

[8] R.L. Workman et al. (Particle Data Group), PTEP **2022**, 083C01 (2022)

[9] L. Tiator, D. Drechsel, S. Kamalov, M. Vanderhaeghen, Chin. Phys. C **33**, 1069 (2009)

[10] G. Eichmann, G. Ramalho, Phys. Rev. D **98**, 093007 (2018), `1806.04579`

[11] A. Kiseleva et al., Indian J. Phys. **85**, 211 (2011)